-Technical Paper-

SEISMIC PERFORMANCE OF UNBONDED POST-TENSIONED PRECAST CONCRETE BEAM-COLUMN CONNECTION

Do Tien THINH[*1], Koichi KUSUNOKI[*2], and Akira TASAI[*3]

ABSTRACT

The aim of this study is to investigate the seismic behavior of the unbonded post-tensioned precast concrete beam-column connections with and without shear bracket under simultaneous action of cyclic load and gravity load. Three specimens of precast unbonded post-tensioned exterior beam-column connection were designed and tested. The test results of the specimen without shear bracket showed excessive beam slip, and large residual deformation. The specimens with shear bracket expressed very good performance with small residual deformation, almost no slip, fully developed strength, minor damage to the beam and column elements, and easy to disassemble. It is concluded that satisfactory seismic performance can be expected from well-designed connection with shear bracket.

Keywords: unbonded, post-tensioned, precast concrete, exterior connection, shear bracket, shear friction

1. INTRODUCTION

From the environmental point of view, the structure should be easy to disassemble when the buildings need to be removed. In order to achieve this purpose, the beam-column joint with un-bonded post-tensioned bars is applied for the proposed system in this paper. As for the ordinary un-bonded post-tensioned (hereafter referred to as PC) joint, the vertical constant load due to the live and dead loads is carried by the friction at the beam-column interface, and bending moment due to lateral load is carried by the PC bars. In office buildings because of its long-span beam, the vertical constant load becomes much larger than that of apartment building. The amount of PC bars for joints at higher stories depends on the vertical load rather than the bending moment, and then larger amount of PC bars tends to be required from the view point of the lateral load resistance. In order to reduce the amount of PC bars, new joint system was proposed in this paper, where the column has a steel bracket on its surface to carry the vertical load of the beam mechanically.

The objectives of this study is design new type of connection in which post-tensioned steel resists the moment induced by seismic and gravity loads, and shear bracket resists the shear force induced by the gravity load. The connection should have well performance at design level of loading, easy and rapid for erecting and disassembling. In order to investigate the performance of the connection, gravity load was applied on the beam together with the cyclic load. This study focuses on the exterior connection in upper stories of a large span frame building. Shear friction behavior of the connection without shear bracket was also investigated.

2. EXPERIMENTAL PROGRAM

2.1 Specimens Outline

The test specimens represent the exterior beam-column connection at the 10th floor of a twelve-story prototype office building, of which story height is four meters and the span length is 18 meters[8]. The demand bending moment and shear force of the beam section at the column face were 86 kNm and 288 kN, respectively. There were three one-half scale specimens in this study. The first, named SP1-A, was designed with shear bracket to resist the shear force induced by the gravity load. The second, named SP2-A, was designed without shear bracket to investigate shear friction mechanism at the beam-column interface. The third, named SP3-A, was designed with shear bracket to resist the gravity load which is one half that of the specimen SP1-A, to investigate the performance of the connection in longer span frame.

2.2 Design of the Specimens

The specimens were designed so that the beam and column reinforcement is still within elastic range and only the PC bar yields. The most critical section was the beam-column interface. In the specimen SP2-A, the PC bars were designed to carry both the demand moment and shear force, while in the specimen SP1-A and SP3-A, the PC bars were designed to carry the demand moment and shear force induced by the seismic load, and the shear bracket resist the shear force induced by the gravity load.

Shear strength of the connection was calculated as:

$$Q_u = \mu.N + Q_b \quad (1)$$

where:

Q_u : shear strength of the connection (N)

*1 Ph.D. Student, Dept. of Architecture, Yokohama National University, JCI member
*2 Associate Professor, Dept. of Architecture, Yokohama National University, Dr. E., JCI member
*3 Professor, Dept. of Architecture, Yokohama National University, Dr. E., JCI member

μ : friction coefficient, $\mu = 0.5$[5]
N : prestressed force (N)
Q_b : shear strength of the bracket (N)

In the case of specimen SP2-A, there is no shear bracket, hence $Q_b = 0$, shear strength of the connection depends only on the shear friction mechanism.

The shear strength of the bracket was calculated as:

$$Q_b = \frac{F_y}{1.5\sqrt{3}} a_w \qquad (2)$$

where:
F_y : yield strength of the steel plate (N/mm^2)
a_w : shear resistance area (mm^2)

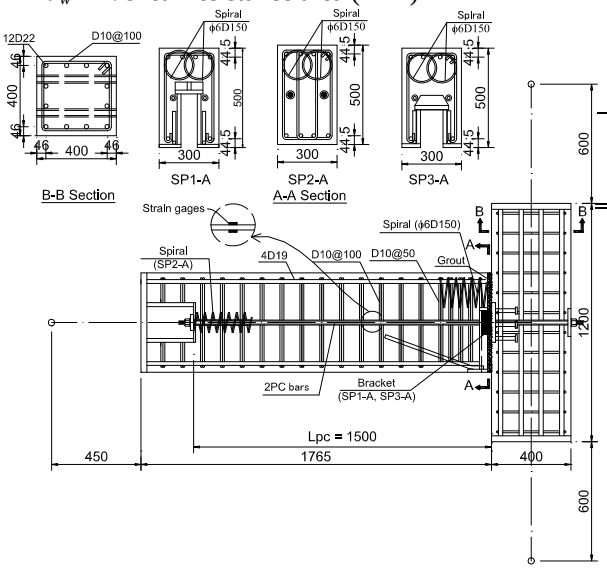

Fig. 1 Reinforcement details of the specimens

Fig. 2 Photos of the shear bracket and U-shaped steel box

The shear bracket in the specimen SP1-A and SP3-A was designed as a corbel welded to a steel plate that anchored to the column by studs. The shear force and moment from the bracket was transferred to the column though these studs. In order to prevent deformation of the bracket and failure of the beam by the concentrated stress at the top face of the bracket touching with the beam, the bracket was designed with T-shaped section to widen the top face area. For the beam socket, in order to prevent failure of the concrete resulted from large compressive stress, the inverted U-shaped steel box was used. Two interlock ϕ6D150 SD295 steel spirals were arranged at the top of the beam end area near the column face to confine the concrete at this position.

Table 1 Specimens outline

Specimens		SP1-A	SP2-A	SP3-A
Beam	Section (mm^2)	300 x 500		
	F_c (N/mm^2)	69.9	60.4	68.6
	f_y (N/mm^2)	339.1	339.1	339.1
	f_{wy} (N/mm^2)	313.1	313.1	313.1
	PC bars	2-ϕ15 Grade C	2-ϕ26 Grade A	2-ϕ15 Grade C
	σ_0(N/mm^2)	1.83	4.02	1.83
	P_0/P_y	0.72	0.72	0.72
	PC length (mm)	1500	1500	1500
Column	Section (mm^2)	400 x 400		
	F_c (N/mm^2)	69.9	60.4	68.6
	f_y (N/mm^2)	534.4	534.4	534.4
	f_{wy} (N/mm^2)	313.1	313.1	313.1
Bracket	a_w (mm^2)	3036	-	4950
	Length (mm)	50	-	50

Where: F_c = concrete compressive strength, f_y = yield strength of beam and column longitudinal reinforcement, f_{wy} = yield strength of beam and column lateral reinforcement, σ_0 = initial concrete beam stress, P_0 = initial prestressed force, P_y = yield strength of the PC bar, a_w = shear resistance area of the bracket.

Brief outline of the test specimens is shown in Table 1, and dimensions and reinforcement details of the specimens is shown in Fig. 1. The photos of the shear bracket and inverted U-shaped steel box are shown in Fig. 2.

2.3 Test Setup

(1) Test setup

The test setup and measuring system is shown in Fig. 3. The cyclic load was applied to the beam end by the 1000 kN vertical hydraulic oil jack connected to the beam end with the pin. The gravity load was applied on the beam as a concentrated load. Because of the restraint of the loading system, the beams of the specimens were shortened from 4.3m to 2.215m. In order to generate the same combination of moment and shear force at the beam column interface as in original condition; the gravity load was controlled by Eqn. (3) according to the original gravity load Q_{L1} and the cyclic load Q_{CY}.

$$Q_L = Q_{L1} + \left(\frac{L_2 - L_1}{L_1 - L'} \right) Q_{CY} \qquad (3)$$

where:
Q_L : actual gravity load
Q_{L1} : original gravity load, = 255 kN for SP1-A, SP2-A, = 382 kN for SP3-A
L_1 : original beam length, L_1 = 4300 mm

L_2 : new beam length, L_2 = 2215mm
L' : distance from the gravity load to the column face, L' = 215 mm
Q_{CY} : cyclic load, Q_{CY} has the same sign with Q_L if they act on the same direction, and vice versa

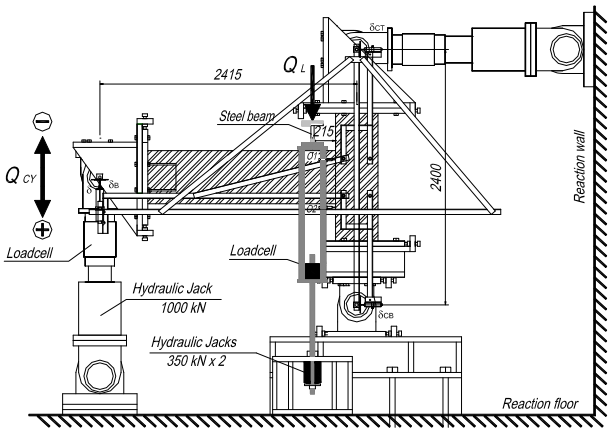

Fig. 3 Test setup

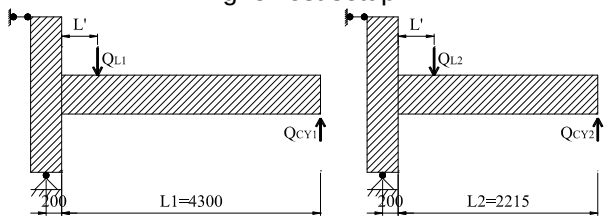

a) Original model b) Actual specimen

Fig. 4 Illustration of the terms in Eq. (3)

(2) Loading history

The first two cycles was loaded by the force control. The peak values were 0.1Q and 0.5Q, where Q is the story shear force that corresponded with yielding of the PC bars. After that, displacement control was used with the peak displacements of 0.25%, 0.5%, 0.75%, 1%, 1.5%, 2%, 3%, 4% drift angle. Two cycles were carried at each story drift level. After finished drift angle of 4%, the test continued as pushover loading up to 6% drift angle in positive direction.

(3) Instrumentation system

The drift angle was measured by the system in that a rigid frame was attached to the pins at the top and bottom of the column and the transducer was fixed on the frame to measure the displacement of the beam at the point applied cyclic load δ. Drift angle was determined as:

$$R = \frac{\delta}{L} \quad (4)$$

where:

R : drift angle (rad)
L : beam length, = 2415 (mm)

Elastic deformation of the beam and column was measured by the system shown in Fig. 3. The curvature of the beam at column face was monitored by two transducers that attached on the beam and targeted on the column. The beam slip was measured by the transducer that was fixed on the column and targeted on the beam in vertical direction. The strains of PC bars, three beam stirrups closest to the column face, four hoops of the column within the joint, and column longitudinal bars were measured using electric resistance strain gauges. The gauges were also used to measure the strain of the inverted U-shaped steel box.

3. TEST RESULTS AND DISCUSSIONS

3.1 Visual Observation

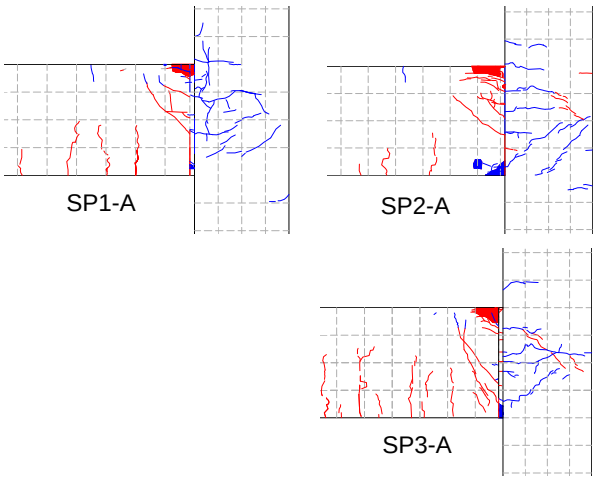

Fig. 5 Crack pattern of specimens after 4% drift

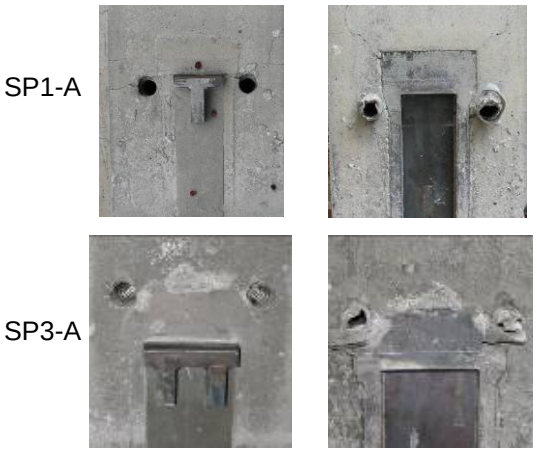

Fig. 6 Shear bracket and beam socket after tested

Fig. 5 shows the crack patterns of the specimens at 4% drift angle. The bracket and beam socket after the test were shown in Fig. 6. Very few cracks occurred in all specimens at story drift of 4%. There was nearly no flexural crack occurred in the columns of all specimens. Only some shear cracks occurred in the joint area with the width less than 0.15 mm and almost closed when the loading was removed. In all specimens, at the story drift of 0.25%, an inclined shear crack occurred from the lower part of the beam to the point of applying gravity load, and stopped to extent at 0.75% drift. At the story drift of 0.07% and 0.12% (SP1-A), 0.09% and 0.2% (SP2-A), 0.09% and 0.15% (SP3-A), decompression occurred in the positive and negative direction, respectively. The crushing of cover concrete at the top of the beam and falling of the grout at the bottom of the beam critical section began at 1.5% drift (SP2-A), and

2% (SP1-A, SP3-A).

As seen in Fig. 6, the shear bracket and beam socket were not suffered from any damage or deformation, although they have experienced very large vertical load and high drift level. Especially in specimen SP3-A where the gravity load was 1.5 times larger than that in other specimens. Furthermore, in the case of specimens with shear bracket, it was very easy to separate the beam out of the column after the test, confirmed that this type of structural is easy to disassemble.

3.2 Hysteresis Behaviour

The test results included the moment and corresponded drift angle at opening, PC yielding, and maximum moment of the specimens, are summarized in Table 2. The hysteresis characteristics of the specimens are shown in Fig. 7 as the relationship between the moment and drift angle.

The vertical axis illustrates the acting moment on the beam at the column face due to the cyclic and concentrated vertical loads and determined as:

$$M = Q_{CY}L - Q_L L' \quad (5)$$

where:

M :acting moment (Nmm)
Q_{CY} : cyclic load (N)
L : beam length, L = 2300 (mm)
Q_L : concentrated vertical load (N)
L' : distance from the concentrated load to the column face, L' = 215mm

The lateral axis illustrates the drift angle, determined by Eqn. (4).

The superimposed dashed lines on Fig. 7 illustrate the hysteresis behavior and modeled as tri-linear skeleton curve. The moment and rotation angle at the breaking points were determined as follow:
The first breaking point:

$$M_s = \frac{1}{2}\left(1 - \frac{\eta_e}{0.85}\right)\eta_e BD^2\sigma_B \quad (6)$$

$$R_s = \frac{M_s}{3EIL} \quad (7)$$

The second breaking point:

$$M_y = \frac{1}{2}\left(1 - \frac{\eta_y}{0.85}\right)\eta_y BD^2\sigma_B \quad (8)$$

$$R_y = \frac{\Delta\varepsilon_{PC}}{0.5D}L_{PC} + \frac{M_y}{3EIL}, \Delta\varepsilon_{PC} = \varepsilon_{py} - \varepsilon_{pe} \quad (9)$$

The end point: $M_u = M_y$.

$$R_u = \frac{\Delta\varepsilon_{PC}}{0.5D}L_{PC} + \frac{M_y}{3EIL}, \Delta\varepsilon_{PC} = \varepsilon_{pu} - \varepsilon_{pe} \quad (10)$$

where:

η_e : = $P_e/BD\sigma_B$
P_e : initial prestress force (N)
B, D : width and height of the beam (mm)
σ_B : concrete compressive strength (N/mm^2)
η_y : = $P_y/BD\sigma_B$
P_y : PC bars yield force (N)
L_{PC} : PC length (mm)
E : Young modulus of the concrete (N/mm^2)
I : second moment of the beam section (mm^4)
L : beam length (mm)
ε_{pe} : initial PC strain (με)
ε_{py} : PC strain at yielding (με)
ε_{pu} : PC strain at ultimate state (με)

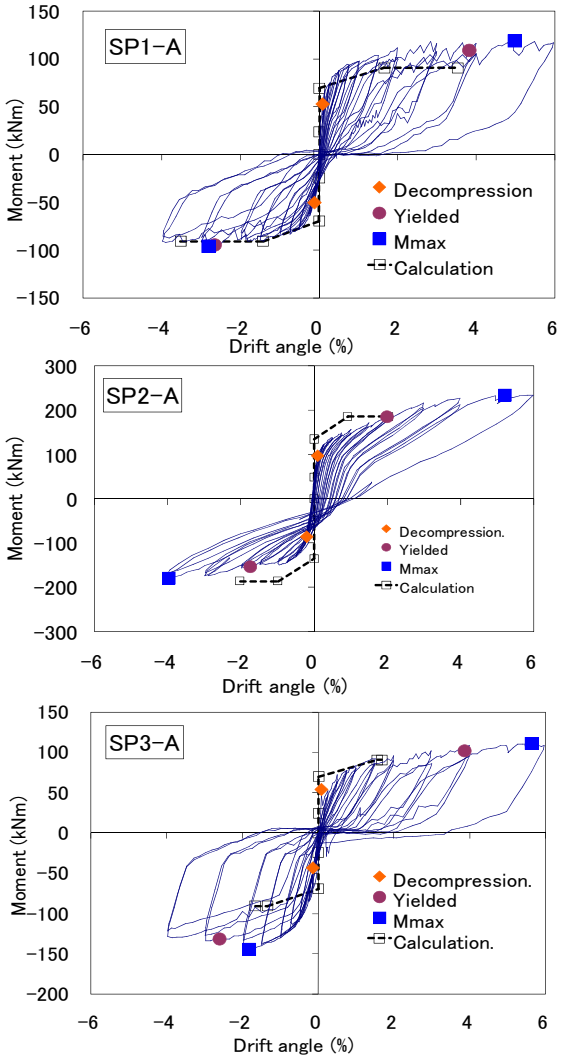

Fig. 7 Moment – Drift angle relationship

All the specimens were successfully passed the drift of 4% in negative directions and 6% in positive direction, and no fracture of PC bars was recorded. As seen in Fig. 7, while the self-centering characteristics of the specimens SP1-A and SP3-A was very good, that of specimen SP2-A was poor. As discussed in the next paragraph, the vertical slip of the beam in the specimen SP2-A was extremely large and was the cause of poor behavior of this specimen.

In the specimen SP1-A, the PC steel was yielded at the drift of 3.82% and 2.65%, and maximum moment strength was reached at the drift of 4.97% and 2.82% in positive and negative direction, respectively. In the specimen SP2-A, the PC steel was yielded at the drift of 1.99% and 1.74%, and maximum moment strength was

Table 2 Summarized test results

Specimens	Loading Direction	M_d (kNm)	R_d (%)	M_y (kNm)	R_y (%)	M_{max} (kNm)	R_{max} (%)	M_y/M_{ycal}
SP1-A	+	52.7	0.09	109.4	3.82	118.7	4.97	1.3
	–	-50.3	-0.12	-94.2	-2.65	-95.4	-2.82	1.1
SP2-A	+	97.1	0.09	185.6	1.99	234.9	5.21	0.99
	–	-84.7	-0.2	-152.5	-1.74	-178.7	-4	0.81
SP3-A	+	53.8	0.07	101.9	3.85	110.9	5.62	1.2
	–	-43.1	-0.15	-132	-2.61	-144.3	-1.82	1.5

Where: M_d, R_d : moment and drift angle when opening occurred; M_y, R_y : moment and drift angle at yielding; M_{max} , R_{max} : maximum moment and corresponded drift angle; M_{ycal}: calculated yielded moment strength.

reached at the drift of 5.21% and 4% in positive and negative direction, respectively. In the specimen SP3-A, the PC steel was yielded at the drift of 3.85% and 2.61%, and maximum moment strength was reached at the drift of 5.62% and 1.82% in positive and negative direction, respectively. In the specimen SP3-A, in the negative direction, the maximum strength was reached at 1.82% drift, before the yielding of the PC steel.

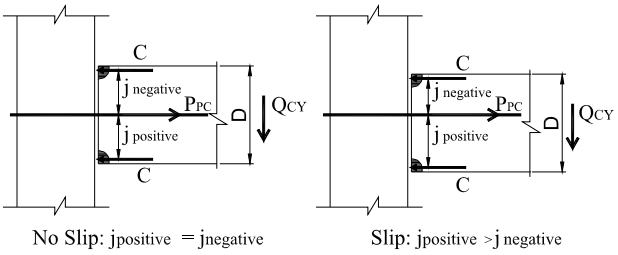

Fig. 8 Illustration of moment strength

In the specimens with shear bracket, yield moment strength well exceeded the calculated values. Average experimental yield moments were 20% and 35% larger for specimens SP1-A and SP3-A, respectively. In the specimen without shear bracket (SP2-A), while the strength in the positive direction was almost the same with the calculated one, it was 20% less than the calculated value in the negative direction. As illustrate in the Fig. 8, when the beam slip occurs, the moment lever arm in the negative direction is smaller than that in the positive direction, causes the moment strength in negative direction smaller than that in the positive direction.

The hysteresis curve well agreed with the computed one in the case of specimen SP1-A. Both the initial and post-yielded stiffness agrees well with the theoretical value. For the specimen SP2-A, the initial stiffness was less than the computed one in negative direction. For specimen SP3-A, the strength in negative direction larger than that in positive direction and much exceeded the calculated value.

3.3 Beam Slip and Friction Coefficient

The beam slip – drift angle relationship of three specimens is shown in Fig. 9. It can be seen that the beam slip of specimen without shear bracket (SP2-A) was excessive larger than that of the specimens with shear bracket (SP1-A and SP3-A). From the test result, it concluded that the shear bracket successfully prevented the slip of the beam. Fig. 10 shows the beam slip and the Q_B/P_{PC} ratio relationship of the specimen SP2-A. The dashed line expresses the upper bound of the ratio of each loading cycle and illustrates the friction coefficient μ. It can be seen that, beam slip occurred when the value of μ was around 0.45. This value is smaller than the design value of $\mu = 0.5$. Further studies are necessary to conducted to find out suitable value of friction coefficient.

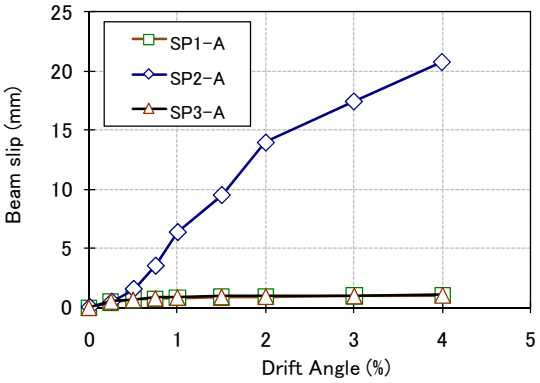

Fig. 9 Beam slip of the specimens

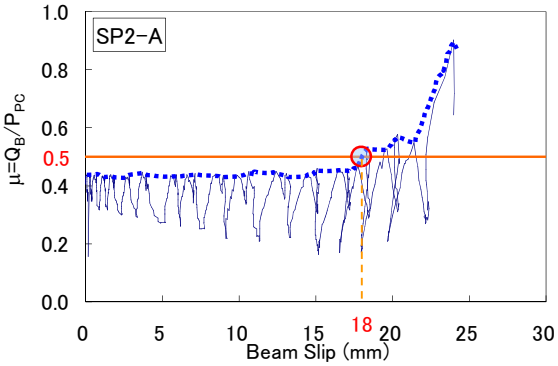

Q_B : Beam end shear force; P_{PC} : PC force

Fig. 10 Beam slip – friction coefficient relationship

3.4 Deflection ratio of the elements

The relationships between the deflections ratio of the elements and the drift angle of the specimens are shown in Fig. 11. The vertical axis expresses the

deflection ratios of the column, beam, and the beam-to-column interface opening rotation to the total deflection. These deflection components were measured by the measuring system shown in Fig. 4. Column deflection was determined as:

$$\delta_C = \delta_{CT} + \delta_{CB} \quad (11)$$

Where δ_{CT} and δ_{CB} were measured by the system shown in Fig. 3.

The average of the deflection ratio of the beam-to-column interface in positive and negative directions at 0.25% drift are 68%, 46.2%, and 65.1% for the specimens SP1-A, SP2-A, and SP3-A, respectively. These values increased up to 86%, 77.6%, and 85.1% for the specimens SP1-A, SP2-A, and SP3-A, respectively at 4% drift. It can be seen that, at large drift angles, total deflection of the specimens mainly contributed by the deflection of the beam-to-column interface. Deflection ratio of the beam-to-column interface of the specimens SP1-A and SP3-A were larger compared to that of the specimen SP2-A, meaning that less deformation occurred to the beam and column elements. This is also one advantage of the connection with shear bracket over the one without shear bracket.

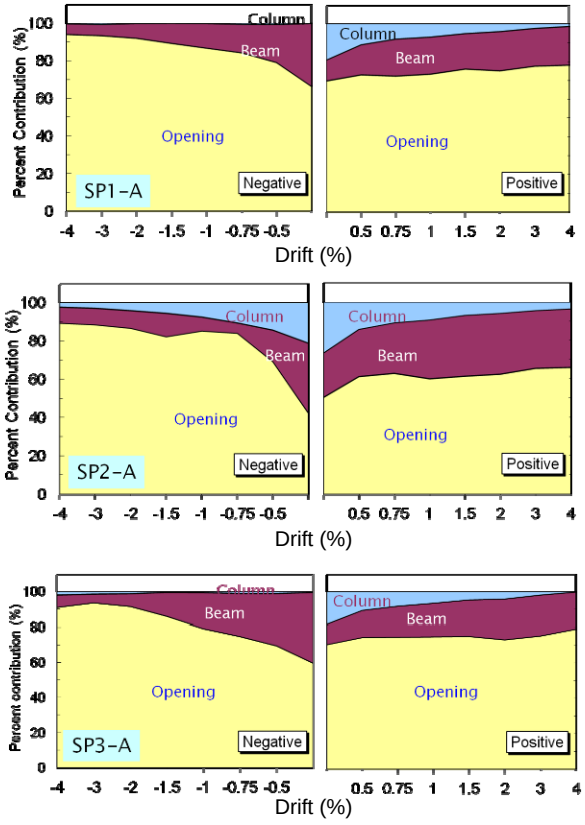

Fig. 11 Deflection ratios of the specimens

4. CONCLUSIONS

Following conclusions was drawn from the experimental results of this study:

1) Shear bracket and beam socket worked well to transfer the shear force from the beam to the column, as well as satisfy the deformability of the beam at high level of drift.

2) The specimens with shear bracket expressed very good seismic performance, with small residual deformation, fully developed strength, nearly no beam slip and small deformation of the beam and column element, even in very long span frame. It is high possibility to apply this type of connection in real precast building structures.

3) The specimens without shear bracket experienced large beam slip and residual drift. The slip occurred at the friction coefficient of 0.45, smaller than design value of 0.5. Performance of the system without bracket was inferior compares to the system with shear bracket.

ACKNOWLEDGEMENT

This research was conducted as a part of the project to develop new type of high-rise R/C office building structure, coordinated by the University of Tokyo and Japan Building Contractors Society, led by Prof. Hitoshi Shiohara. The finance was funded by Japan Ministry of Land, Infrastructure and Transport.

REFERENCES

[1] D. T. Thinh, K. Kusunoki, and A. Tasai, “Study on a New Precast Post-Tensioned Beam-Column Joint System for Rapid Erection and Improved Resiliency”, JCI Annual Convention, 2008.

[2] D. T. Thinh, K. Kusunoki, and A. Tasai, “Experimental Study on a New Precast Post-Tensioned Concrete Beam Column Connection System”, 14th World Conference on Earthquake Engineering, 2008.

[3] S. Pampanin, A. Amaris, and A. Palermo, “Implementation and Testing of Advanced Solutions for Jointed Ductile Seismic Resisting Frames,” Federation International du Beton, Proceeding of the 2nd International Congress, June 5-8, 2006, Naples, Italy.

[4] M. J. N. Priestley, and J. Tao, “Seismic Response of Precast Prestressed Concrete Frames with Partially Debonded Tendons,” PCI JOURNAL, Vol. 38, No. 1, January-February 1993, pp. 58-69.

[5] Architecture Institute of Japan, “Standard for Structural Design and Construction of Prestressed Concrete Structures”, 2004

[6] Prestressed Concrete Institute, “PCI Design Handbook”, 6th Edition, 2004.

[7] W. C. Stone, G. S. Cheok, and J. F. Stanton, “Performance of Hybrid Moment-Resisting Precast Beam-Column Concrete Connections Subjected to Cyclic Loading,” ACI Structural Journal, V91, No.2, March-April 1995.

[8] H. Shiohara, O. Chiba, "Development of a Large-Span Precast Concrete Structural System with Ease of Construction Using Prestressed Connections, Part 1: Objectives and the Research Program", AIJ Annual Convention, September, 2008, pp 651-652.